A BIRD'S-EYE VIEW

Development of an Operational ARM Unmanned Aerial Capability for Atmospheric Research in Arctic Alaska

Gijs de Boer, Mark Ivey, Beat Schmid, Dale Lawrence, Darielle Dexheimer, Fan Mei, John Hubbe, Albert Bendure, Jasper Hardesty, Matthew D. Shupe, Allison McComiskey, Hagen Telg, Carl Schmitt, Sergey Y. Matrosov, Ian Brooks, Jessie Creamean, Amy Solomon, David D. Turner, Christopher Williams, Maximilian Maahn, Brian Argrow, Scott Palo, Charles N. Long, Ru-Shan Gao, and James Mather

Unmanned aerial capabilities offer exciting new perspectives on the Arctic atmosphere.

The Arctic climate system is evolving at a rapid pace. Surface- and satellite-based observations show increasing temperatures (Simon et al. 2005; Rigor et al. 2000; Serreze and Francis 2006), decreasing sea ice (Kwok and Untersteiner 2011; Maslanik et al. 2011; Lindsay and Schweiger 2015), thawing permafrost (Romanovsky et al. 2002), and changing ecosystems (Burek et al. 2008; Post et al. 2013). It is believed that the changes observed in the Arctic are the result of "Arctic amplification" (e.g., Serreze and Barry 2011; Pithan and Mauritsen 2014), an accelerated warming of the northern polar region resulting from a combination of various climate feedbacks (Screen and Simmonds 2010; Pithan and Mauritsen 2014; Döscher et al. 2014). Central to several of these feedbacks are physical relationships involving clouds, aerosols, and atmospheric and surface states, and their combined effect on radiative transfer in the global climate system.

Models across a variety of scales have been shown to struggle with the representation of processes relevant to the simulation of these critical drivers of radiative transfer (Stroeve et al. 2007, 2012; Miller et al. 2018). In particular, the roles of Arctic thermodynamic structure, aerosols, clouds, and the connections between them have proven to both be problematic for models (e.g., de Boer et al. 2012) and result in divergence of projections for future scenarios (e.g., Chylek et al. 2016). Misrepresentation of these processes impacts simulations of surface and top-of-

AFFILIATIONS: de Boer, Shupe, Telg, Matrosov, Creamean, Solomon, Williams, Maahn, and Long—University of Colorado Boulder, and NOAA/Earth System Research Laboratory, Boulder, Colorado; Ivey, Dexheimer, Bendure, and Hardesty—Sandia National Laboratories, Albuquerque, New Mexico; Schmid, Mei, Hubbe, and Mather—Pacific Northwest National Laboratory, Richland, Washington; Lawrence, Argrow, and Palo—University of Colorado Boulder, Boulder, Colorado; McComiskey, Turner, and Gao—NOAA/Earth System Research Laboratory, Boulder, Colorado; Schmitt—National Center for Atmospheric Research, Boulder, Colorado; Brooks—University of Leeds, Leeds, United Kingdom
CORRESPONDING AUTHOR: Gijs de Boer, gijs.deboer@colorado.edu

The abstract for this article can be found in this issue, following the table of contents.
DOI:10.1175/BAMS-D-17-0156.1

In final form 7 March 2018

the-atmosphere energy budgets, resulting in errors impacting the representation of land and sea ice processes, which in turn impact the climate feedbacks discussed above. Additionally, deposition of aerosol particles on snow and ice can change surface reflectivity and melt rates (e.g., Hansen and Nazarenko 2004), driving a need for aerosol source attribution and characterization of transport pathways.

Since 1997, the U.S. Department of Energy's (DOE) Atmospheric Radiation Measurement (ARM) program (Turner and Ellingson 2016) has collected measurements of clouds, aerosols, the atmospheric state, and radiation in northern Alaska. These measurements started at the heavily instrumented North Slope of Alaska (NSA) observatory, located in Utqiaġvik (formerly Barrow; Verlinde et al. 2016). For a little over 10 years (1999–2010), ARM also operated an auxiliary observatory roughly 60 mi (~97 km) inland from Utqiaġvik at Atqasuk to collect information on spatial variability between the nearshore and inland environments in Arctic Alaska.

These observatory-based measurements have supported tremendous advancement of our understanding of the Arctic natural system. This includes work to understand cloud properties and their radiative impact (e.g., Kay et al. 2008; Dong et al. 2010, Cox et al. 2016), interactions between aerosols and clouds (e.g., Penner et al. 2004; Lubin and Vogelmann 2006; Garrett and Zhao 2006), and Arctic aerosol properties (e.g., Quinn et al. 2002; Quinn et al. 2009; McComiskey and Ferrare 2016). Such studies have resulted in the evaluation of and improvements to numerical models across various scales (e.g., Xie et al. 2006; Morrison et al. 2009; de Boer et al. 2012). When put into the context of a larger observational network, such as that provided by the International Arctic Systems for Observing the Atmosphere (IASOA; Uttal et al. 2016) consortium, such results provide a pan-Arctic synthesis to inform questions related to the spatial variability of the atmosphere and its interactions with the surface (e.g., de Boer et al. 2011; Shupe 2011; Shupe et al. 2011).

Despite these advances, other studies have demonstrated a continued need for new perspectives. For example, work to help understand interactions between aerosols and clouds at high latitudes has been hampered by a general lack of vertical profiling of aerosol properties. Given Arctic atmospheric stratification, it is not clear that aerosol properties measured at the Earth's surface are connected to clouds at any given time (e.g., Shupe et al. 2013). Yet important studies detailing relationships between aerosols and clouds have only had access to surface-based measurements (e.g., Garrett and Zhao 2006; Lubin and Vogelmann 2006). Similarly, efforts to understand the seasonal variability in aerosol loading throughout the Arctic atmospheric column, and the disparate sources responsible for such loading, have only limited airborne datasets from which to draw conclusions. Yet such a vertical distribution represents a significant factor in determining the radiative impact of the particles. Similarly, cloud properties are only indirectly observed with ground-based remote sensing instrumentations and in situ observations are required to study cloud processes in detail. Therefore, additional information on the vertical profiles of aerosol and cloud properties is required.

In addition to understanding the vertical structure, questions exist about horizontal variability. As an example, the representativeness of surface radiation and turbulent flux measurements at the regional scale are a consideration. Generally, at any given site, instrumentation deployed by ARM collects these measurements at a single location. Additionally, while ARM instrumentation has been deployed in coastal locations, it is difficult to say how relevant such measurements are to the Arctic overwater (or sea ice) environment. Such information is crucial to understanding how this ice pack is evolving over time. A couple of recent studies (Maahn et al. 2017; Creamean et al. 2017) demonstrate the spatial variability of aerosol properties along the north slope of Alaska and the response of cloud properties to these gradients. However, these results focus on a short time period (summer 2016) due in part to the cost and effort associated with airborne in situ measurements.

To gain these perspectives, the DOE ARM program recognized many years ago the potential for unmanned aircraft, developing the ARM Unmanned Aerial Vehicle (ARM UAV) program in the early 1990s (Schmid et al. 2016). In collaboration with industry partners, this program supported various pioneering midlatitude campaigns throughout the 1990s and into the early 2000s (Stephens et al. 2000), deploying larger, expensive unmanned aircraft systems (UASs). Even before these efforts, UASs were developed to do things like deploy dropsondes (Langford and Emanuel 1993), conduct routine profiling flights (Holland et al. 1992), and survey atmospheric transects (Holland et al. 2001). Initial Arctic flights flown in conjunction with the ARM program were conducted from Barrow using the Aerosonde platform (Curry et al. 2004). Since then, use of these systems has expanded tremendously, thanks in part to continued component cost and size reductions by industries targeting consumer

electronics (i.e., cellular "smart" phones). Research has been conducted through both high-latitude (e.g., Cassano et al. 2010; Knuth and Cassano 2014) and lower-latitude (e.g., Corrigan et al. 2006; Ramanathan et al. 2007; Van den Kroonenberg et al. 2008; Houston et al. 2012) deployments.

In addition to the use of UASs, the atmospheric science community has for many years deployed tethered balloon systems (TBSs) for profiling the lower atmosphere. These systems range widely in size and can carry payloads of up to several kilograms. They offer the benefit of extended flight times during times of good weather conditions, but fall short of the UASs in terms of flexibility when sampling a targeted spatial location or in capturing gradients across boundaries. Example applications include the measurement of atmospheric composition and structure (e.g., Greenberg 1999; Pisano et al. 1997; Neff et al. 2008; Shupe et al. 2012) and cloud microphysical properties (e.g., Duda et al. 1991; Kitchen and Caughey 1981; Zhang et al. 1997).

INITIAL PROGRESS TOWARD ROUTINE OBSERVATIONS. In recognition of the potential for unmanned aerial measurements from both UASs and TBSs to provide the perspectives described above, in 2013 the DOE ARM program deployed its third ARM mobile facility (AMF-3) to Oliktok Point, Alaska, approximately 260 km to the east-southeast of Utqiaġvik. This deployment was conducted in part to provide detailed, continuously operating observations at a site where DOE manages special-use airspace (e.g., R-2204 and W-220; de Boer et al. 2016a) for operation of aircraft and balloon systems. Given the availability of airspace at Oliktok Point, ARM has moved toward development, support, and operation of their own unmanned aerial capability, with an eye toward routine Arctic sampling. This includes the operation of UASs and TBSs, along with procurement of cutting-edge miniaturized instrumentation to support Earth system science. Additionally, it includes the development of infrastructure to provide complementary ground-based measurements, offer housing and shelter for campaign participants, and process data collected in an efficient manner to quickly stream datasets for public consumption through the ARM data archive. In this article, we provide information on work that has helped to shape this capability, provide information on instrumentation and infrastructure, and offer example data and perspectives on future directions.

Oliktok Point's unique ability to provide access for UAS-based atmospheric measurements over tundra, water, and ice, along with the (then) low volume of local air traffic, were identified in early discussions with the Federal Aviation Administration (FAA), North Slope oilfield operators, and local aviators. Such discussions resulted in the establishment of special-use airspace (R-2204), a 2 nautical mile (n mi, 1 n mi = 1.852 km) radius cylinder centered on Oliktok Point that extends to 7,000 ft (2,134 m) above mean sea level (MSL), at Oliktok Point in 2004. Since then, amendments were approved to segment R-2204 into low [surface to 1,500 ft (457 m) MSL] and high (1,500–7,000 ft MSL) sections and to increase the number of activation days from 30 to 75 per year. Activation of R-2204 closes airspace to aviation operations except those authorized by the DOE via Sandia National Laboratories.

In addition to R-2204, Warning Area W-220 was established in 2015. W-220 provides an area suitable for scientific operations while reducing hazards to routine air traffic. W-220, which starts 12 n mi offshore, is 40 n mi wide, 673 n mi long, and extends from the surface to, but not including, 10,000 ft (3,048 m) MSL. Like R-2204, W-220 is divided into two altitude segments, [surface–2,000 (610 m) and 2,000–10,000 ft MSL]. W-220, bounded between 70°47′ and 82°N, has eight segments ranging from 50 to 173 n mi in length that may be individually activated. W-220 occupies international airspace in the U.S.-controlled Anchorage Flight Information Region (FIR). Maps illustrating the location of Oliktok Point and the extent of both R-2204 and W-220 are included in Fig. 1.

Since W-220 was established in 2015, several UAS flights have included UAS transits between R-2204 and W-220. The Department of Energy has worked with the FAA Anchorage Flight Control Center and used the FAA certificate of authorization (COA) process to identify safe and effective ways to manage transit flights for different UAS platforms and missions. Initial transit flights between R-2204 and W-220 used an altitude reservation corridor (ALTRV) together with local air traffic information obtained from radar systems. In one case, a flight-certified radar was deployed temporarily at Oliktok Point. For another set of flights, DOE staff were provided access to real-time air traffic information systems in Anchorage to help monitor regional air traffic and ensure a safe transit between R-2204 and W-220.

Several ongoing efforts make it likely that FAA approvals for transits between R-2204 and W-220 and beyond-line-of-sight (BLOS) operations will be easier in the future. This includes work with the FAA to get

ready access to local air traffic information at Oliktok for flight information purposes. In 2012, Congress directed the FAA to establish permanent areas in the Arctic that provide UASs with "ingress and egress routes from selected coastal launch sites at least 2,000 feet in altitude." It is believed that Oliktok Point will be one of these coastal launch sites where ingress and egress routes can be established under FAA guidance to ease safety case development and approvals.

Initial flights. Since its establishment, R-2204 has been used numerous times for UAS and TBS operations. A list of recent flight campaigns (since 2014) is included in Table 1, with the campaigns color coded to match flight paths indicated in Fig. 1. R-2204 was first used for TBS flights during the 2004 Mixed-Phase Arctic Cloud Experiment (M-PACE; Verlinde et al. 2007). After M-PACE, additional TBS science flights were conducted during the Arctic Lower Troposphere Observed Structure (ALTOS; Verlinde 2010) campaign, and in an engineering and evaluation capacity by New Mexico State University in 2012. Around this time, the DOE ARM and Atmospheric Systems Research (ASR) programs jointly funded science and evaluation flights under the Evaluation of Routine Atmospheric Sounding Measurements using Unmanned Systems (ERASMUS) project. These flights were designed to demonstrate some unique perspectives obtainable using UASs and to evaluate the feasibility of routine flight operations in the harsh Arctic environment. As a run-up to ERASMUS, a small team of researchers visited Oliktok Point with a first-generation University of Colorado (CU) DataHawk aircraft (Lawrence and Balsley 2013) to

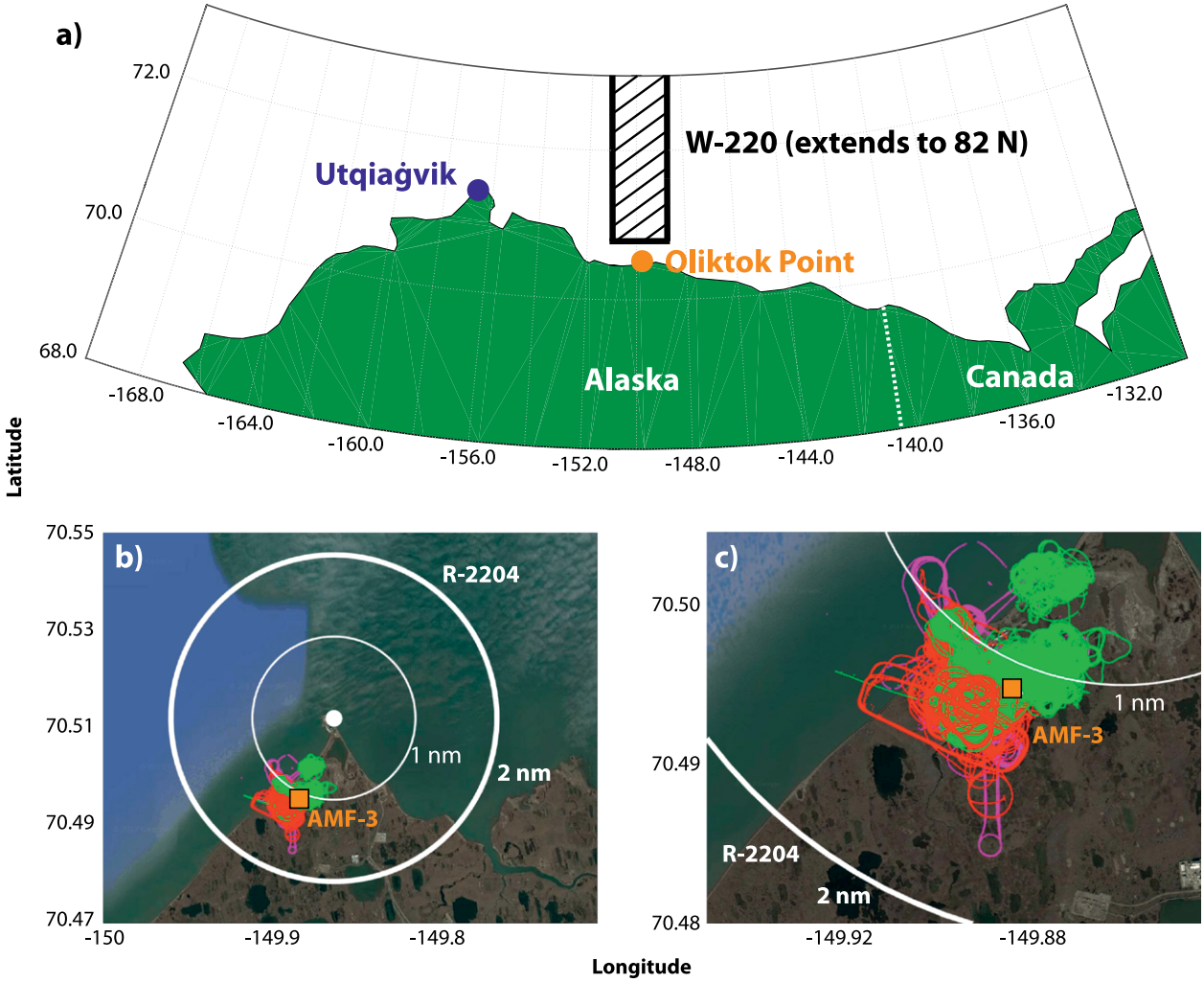

Fig. 1. (a) Maps of the NSA including W-220 and the locations of Oliktok Point and Utqiaġvik. (b) The Oliktok Point region including the extent of R-2204 (white), the location of the AMF-3 (orange), and flight campaign flight tracks color coded relative to Table 1. (c) A close-up of campaign flight tracks and the location of the AMF-3.

conduct initial flights alongside a tethered balloon operated by ARM. This effort, referred to as Coordinated Observations of the Lower Arctic Atmosphere (COALA), included two weeks of flight activities in mid-October 2014 during a time of transition and sea ice formation, and resulted in the first succesful ARM-supported science flights using small UASs at Oliktok Point and the first coordinated UAS–TBS flight activity there. In total 6.5 flight hours were conducted over 29 flights as part of COALA in R-2204 (Fig. 1), resulting in measurements of atmospheric thermodynamic properties and surface temperature. Despite strong winds and aircraft icing conditions, the campaign was conducted successfully and safely, laying groundwork for more extensive flights for ERASMUS.

ERASMUS. ERASMUS represented the first DOE-funded, scientific UAS campaign at Oliktok Point. It included three campaign periods, with the CU DataHawk2 (DH2) deployed in August 2015, the CU Pilatus (de Boer et al. 2016b) deployed in early April 2016, and the CU DH2 deployed again in October 2016. The August DH2 flights revealed a previously unidentified challenge in Oliktok Point operations: electromagnetic interference (EMI) from the U.S. Air Force North Warning System (NWS) Oliktok Point Long Range Radar. Unfortunately, this EMI limited autopilot flight operations and required frequent manual pilot operation of the aircraft. With this limitation, 159 DH2 flights were conducted totaling 22.3 flight hours. This included regular (hourly) profiling of the lower atmosphere between 0800 and 1800 Alaska daylight saving time (AKDT).

After conducting TBS-based EMI testing on the DH2 and Pilatus autopilot systems, the ERASMUS team returned with the Pilatus during 2–16 April 2016. The Pilatus flights were meant to demonstrate more advanced measurement capabilities, including profiling of aerosols and broadband irradiance, while simultaneously expanding operations to cold, early spring conditions. While the cold (–10° to –20°C) did not pose major issues, anomalously strong winds resulting from a persistent Beaufort high did limit flight operations. After waiting out two consecutive weeks of 25 mi h^{-1} (~40 km h^{-1}) or greater surface winds, the campaign was briefly extended to complete six science flights with the Pilatus (1.4 flight hours). These flights and precampaign preparations provided valuable information on the deployment of broadband radiometric instruments on small UASs. For shortwave (SW) measurements, correction for tilt from horizontal is necessary to obtain accurate downwelling irradiance measurements. Such corrections (Long et al. 2010) were applied to the Pilatus's fast-response (0.3 s, 95%) sensors to

Table 1. An overview of flight campaigns for COALA, ERASMUS, and ICARUS. Colors match those used in the map in Fig. 1.

Campaign	Dates	Operator	Platforms	No. of flights (UAS/TBS)	No. of flight hours (UAS/TBS)
COALA	6 –20 Oct 2014	CU, DOE ARM	DH1, TBS	29/3	6.5/5
ERASMUS	2–16 Aug 2015	CU	DH2	206/0	41/0
	2–16 Apr 2016	CU	DH2, Pilatus		
	9–22 Oct 2016	CU	DH2		
ICARUS	22–28 Oct 2015	DOE ARM	TBS	130/55	77.8/198
	3–20 Apr 2016	DOE ARM	TBS		
	5–11 Jun 2016	DOE ARM	DH2, TBS		
	26 Jun–27 Jul 2016	DOE ARM	DH2, TBS		
	25–26 Sep 2016	DOE ARM	TBS		
	9–22 Oct 2016	DOE ARM	TBS		
	15–17 Nov 2016	DOE ARM	TBS		
	2–9 Apr 2017	DOE ARM	TBS		
	14–28 May 2017	DOE ARM	DH2, TBS		
	1–15 Aug 2017	DOE ARM	DH2, TBS		
	12–24 Oct 2017	DOE ARM	TBS		

measure direct and diffuse irradiance, along with broadband albedo. Unfortunately, the longwave (LW) pyrgeometers deployed were too slow for UAS applications (18 s, 95%), demonstrating a need for the development of faster-response LW instrumentation. Additionally, methodologies for characterizing sensor angular offset from the system's inertial navigation system, as needed for tilt correction (Long et al. 2010;

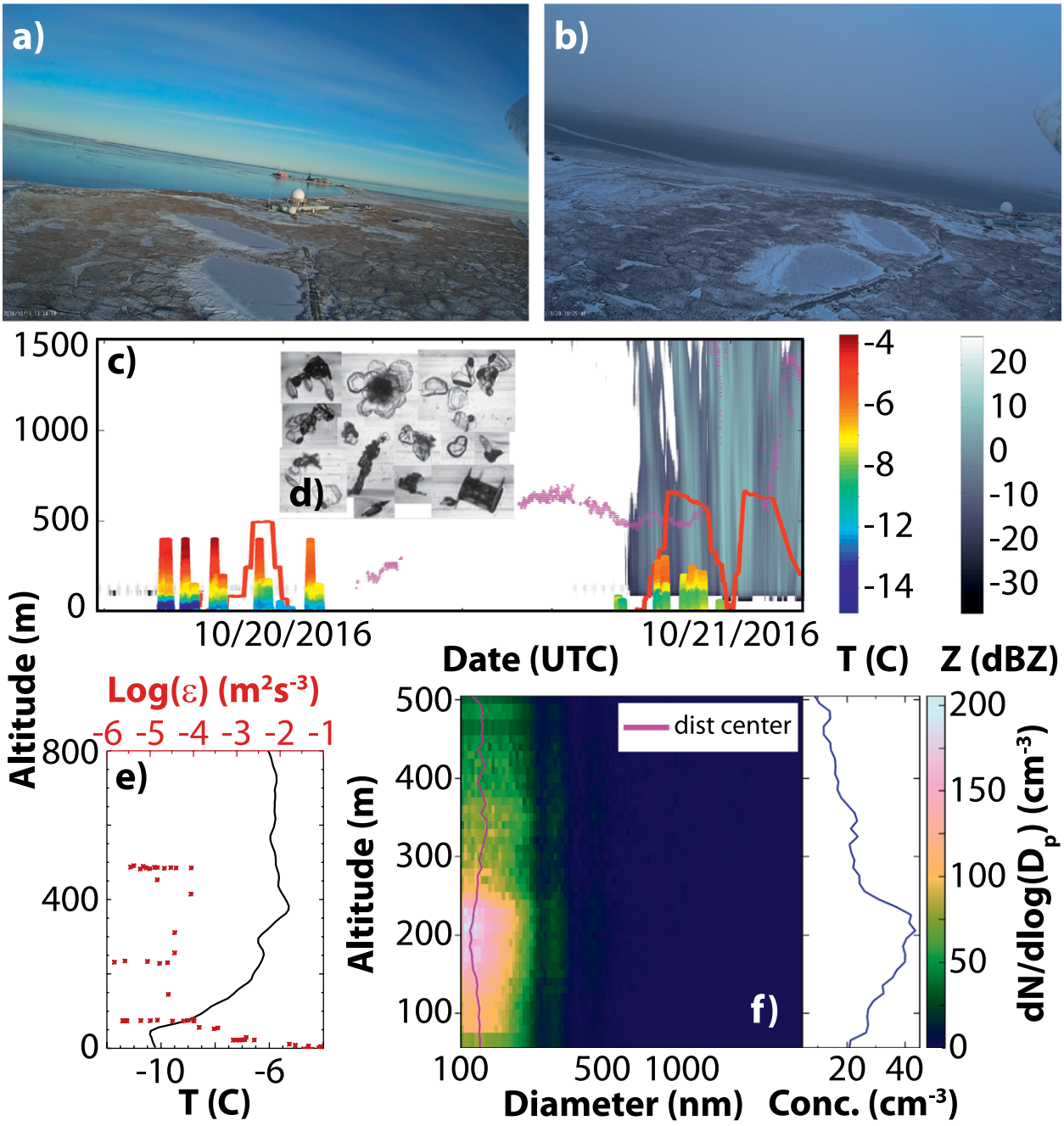

Fig. 2. An example of measurements collected by the DH2s and TBS system on 19–21 Oct 2016. (a),(b) The photos show the contrasting conditions observed from the eyes of the DH2, with 19–20 Oct being a clear, cold day, and 20–21 Oct featuring cloud cover. (c) The time series includes the temperature structure from DH2 flights (*T*, colored contouring), radar reflectivity from the KAZR radar (*Z*, grayscale), cloud base from the ceilometer (magenta dots), and the TBS flight tracks (red dots). (d) Inset illustrates ice crystals imaged with the VIPS on 21 Oct. (e) Temperature *T* and turbulent dissipation rate ε from the TBS-mounted sonic anemometer on 20 Oct. (f) Aerosol properties observed by POPS on 21 Oct. The pink line in the POPS figure ("dist center") represents the center position of a lognormal distribution that has been fit to the observed particle number size distribution.

de Boer et al. 2016b), were developed specifically for UAS applications.

In addition to the broadband instrumentation, Pilatus was the first platform to deploy the Printed Optical Particle Spectrometer (POPS; Gao et al. 2016) at Oliktok Point. This instrument, originally developed in the National Oceanic and Atmospheric Administration's (NOAA) Chemical Sciences Division (CSD), provides aerosol size distributions for particles between 140 and 3,000 nm and was previously deployed on UASs at Ny Alesund, Norway (Telg et al. 2017). This instrument performed well during ERASMUS, motivating ARM to acquire POPS instruments from its commercial supplier for ARM operations. Examples of POPS measurements from TBS flights are included in Fig. 2f, and include a vertical profile of the particle size distribution and a profile of the center of a lognormal distribution fit to the observed distribution (pink line). This particular case offers a nice example where surface-based aerosol measurements were not necessarily representative of conditions at and below the cloud layer. A strong temperature inversion resulted in a decoupled cloud, with near-surface aerosol concentrations substantially lower than those in the heart of this inversion around 200 m. The physical processes responsible for the observed accumulation of aerosols within the inversion layer and the related shifts in particle size distribution are currently under investigation.

With DH2 autopilot hardening complete, a final ERASMUS deployment was conducted from 2 to 16 October 2016, resulting in the completion of 41 autopilot-controlled flights (17.3 flight hours). This improved system performance was important for ARM because the program acquired four DH2 UASs under ERASMUS. Conducted in tandem with TBS operations associated with the Inaugural Campaigns for ARM Research Using Unmanned Systems (ICARUS; see the next section), these flights provided a detailed dataset, including DH2-based measurements of well-mixed and stable boundary layers, the cloud-driven mixed layer, and surface turbulent fluxes over various surfaces. Examples of temperature profiling from these flights are included in Fig. 2c (colored contours) and a demonstration of their use for evaluation of retrievals and models is included in Fig. 3. While similar comparisons could be done using radiosonde-based sensors, cost considerations limit the number of sondes that can be launched, limiting information on temporal variability at scales of minutes to hours. In addition to the thermodynamic profiling, the DH2 performed a series of low-altitude (15–20 m) offshore flights over newly forming sea ice to measure the temperature, moisture, and winds from which to calculate sensible and latent heat fluxes (Fig. 4). This figure illustrates the aircraft flight track along the shore, along with the variables needed to calculate the sensible heat flux over newly forming sea ice from this flight. This broken and thin ice environment provides a striking example of previously unobtainable measurements provided by UASs, as deployment of traditional sensors associated with towers and buoys would not necessarily be feasible in this dynamic and unstable surface environment.

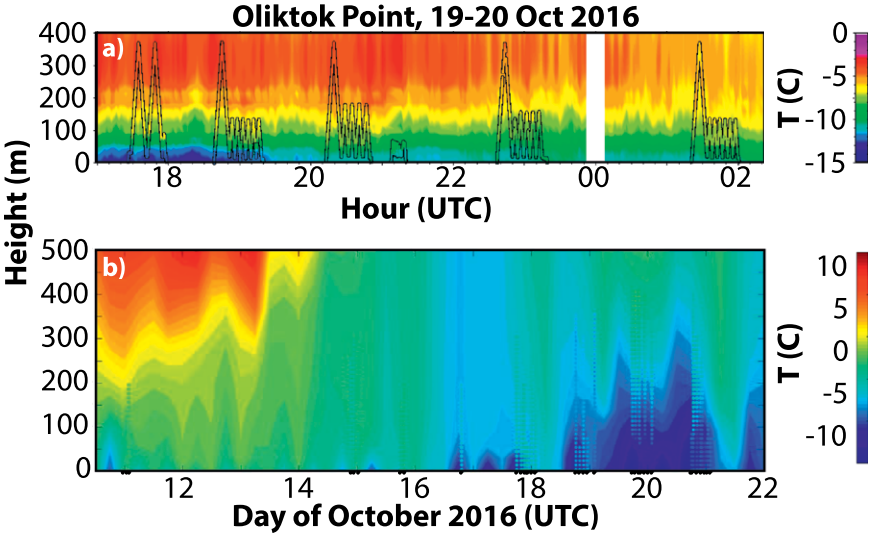

Fig. 3. Examples of (a) the use of ERASMUS DH2 data in the evaluation of remote sensing retrievals and (b) model output. In (a) DH2 profiles of temperature (lines) are compared with the retrievals from the Atmospheric Emitted Radiance Interfereometer (AERI; Turner and Löhnert 2014; background shading) at Oliktok Point during the erosion of a stable boundary layer. In (b) DH2 temperature measurements (dots) are compared with temperature output from the NOAA/Earth System Research Laboratory (ESRL) branch of the Regional Arctic System Model (RASM-ESRL, shading) that is being used for sea ice forecasting. The small black dots along the x axis in (b) indicate DH2 flight times.

Ongoing work. With the ARM program acquiring UAS (DH2) and TBS systems for programmatic operations, plans were developed for initial engineering and evaluation flights under DOE operational control. To make such flights as useful as possible for both the ARM operations and DOE scientific communities, a joint workshop was held including ARM operators and scientists and the ASR-funded Oliktok Point site science team. The initial workshop, held in Boulder, Colorado, in January 2016, included discussions to help find intersections between scientific priorities and operational feasibility, and resulted in the development of an operational plan for ICARUS DH2 and TBS operations. After successful 2016 deployments, a similar workshop was held in January 2017 to revise and adjust plans for the current season based on lessons learned in 2016. Priorities emerging from these workshops included profiling of atmospheric thermodynamics, profiling of aerosol properties, profiling of cloud micro- and macrophysical properties, evaluation of spatial variability in surface temperature and turbulent surface fluxes, and evaluation of sensor performance across a variety of conditions.

ICARUS. Through the fall of 2017, there have been 55 and 130 flights of the ARM TBSs and UASs as part of ICARUS, resulting in 198 and 77.8 flight hours for these platforms, respectively. As an example of the types of measurements obtained, the frequency and seasonal coverage of ICARUS flights have provided thermodynamic profiles for the statistical evaluation of models and retrieval algorithms and have included joint UAS–TBS flights combining a variety of atmospheric instruments (Fig. 2). Additionally, TBS-based deployment of a Distributed Temperature Sensing (DTS; Tyler et al. 2009) system, which uses a fiber-optic cable to provide high-resolution measurements of atmospheric temperature, provides detailed information on lower-atmospheric structure. This system will allow for future evaluation of theoretical thermodynamic structures produced in high-resolution simulations of the stable boundary layer (e.g., Sullivan et al. 2016).

Another priority for ARM has been to conduct routine vertical profiling of aerosols to better understand the representativeness of surface-based aerosol measurements in the Arctic and provide contextual measurements for studies of aerosol–cloud interactions. Doing so provides insight into long-range transport and aerosol layering and their relationships to atmospheric stratification. Aerosol profiling during ICARUS involved TBS-based measurements of aerosol size distributions using the POPS. Additionally, condensation particle counters

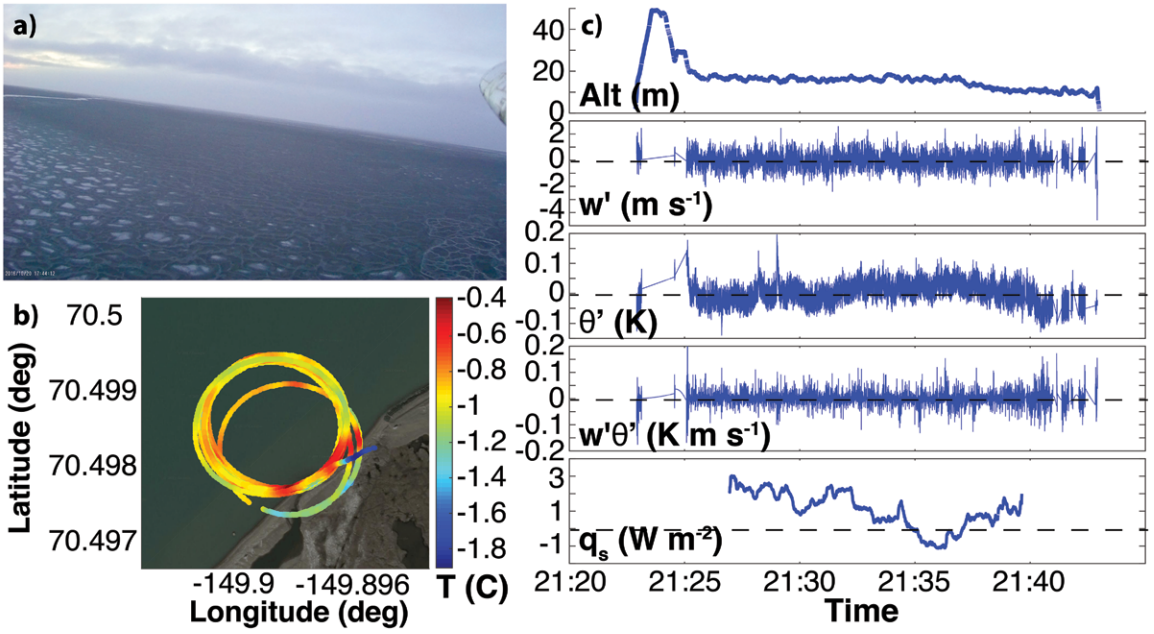

Fig. 4. An example of a DH2 flight used to estimate sensible heat flux over newly forming sea ice. Included are (a) a photo taken from the DH2 as it flies at 20 m over the thin sea ice; (b) the aircraft flight track, color coded by surface temperature; and (c) time series of altitude (Alt), vertical velocity anomaly w', potential temperature anomaly θ', the product of these two ($w'\theta'$), and the calculated sensible heat flux from this flight q_s. The mean air temperature measured for this time period was −2.12°C and the mean wind speed was 3.2 m s^{-1}.

(CPC3007, TSI, Inc.) were deployed alongside POPS during 2017 to measure particles with diameters from 10 to >1,000 nm. Figure 5 illustrates the potential for stratification of the Arctic atmosphere and associated aerosol particles surrounding cloud features, with POPS and CPC measurements revealing an elevated aerosol layer existing above a stratiform cloud layer, illustrated by contours of radar reflectivity (grayscale) and ceilometer cloud base (magenta dots) observed on 23 May 2017. Observing such stratification raises a variety of questions related to the cloud processing of aerosol, the sources of cloud condensation and ice-forming nuclei, and possible contamination of relationships derived from investigations of aerosol–cloud interactions at high latitudes using surface-based aerosol instrumentation. In this specific case, the fact that the elevated aerosol layer is associated with a warmer, drier air mass may indicate that these aerosol particles were transported into the Arctic from lower latitudes.

In addition to understanding the aerosol structure, the TBS platform provides opportunities for characterizing the structure of Arctic clouds. Of primary importance in dictating the radiative influence of the cloud is the amount and vertical distribution of the liquid water. The TBSs have been equipped with sensors to provide information on liquid water content, which use vibrating wires to evaluate water concentrations (Hill and Woffinden 1980). These sensors can provide information on the adiabaticity of various Arctic cloud types and can help with the evaluation and improvement of remote sensor retrievals of liquid cloud properties. Additionally, relative humidity sensors provide guidance on cloud boundaries, along with ground-based instrumentation deployed as part of the AMF-3.

One process responsible for governing liquid water amounts in climatically important mixed-phase clouds is the removal of water from the cloud layer by ice crystal precipitation. The rate of such removal is governed in part by crystal shape (or habit), making information on the frequency of occurrence of these habits critical to representing these clouds in atmospheric models. New dual-frequency (35 and 94 GHz) scanning ARM cloud radars (SACRs) and updated Ka-band (35 GHz) ARM zenith-pointing radars (KAZRs) were deployed at different ARM facilities (Kollias et al. 2016), including the AMF3 at Oliktok Point. These radars have polarimetric capabilities that offer possibilities for the estimation of mean crystal shape in terms of particle aspect ratios. To evaluate the ability of polarimetric radar retrievals to determine the aspect ratio, the October 2016 ICARUS TBS

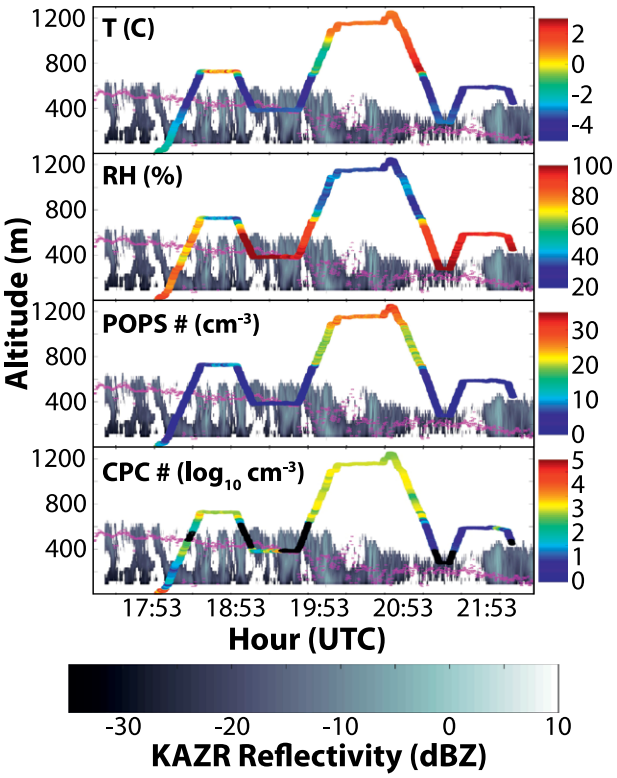

Fig. 5. TBS-obtained vertical profiles of (from top to bottom) temperature, relative humidity, aerosol concentration for particles in the POPS size range, and total aerosol number concentration from the CPC. The grayscale contours represent radar reflectivity, and the magenta dots represent the cloud base from the AMF-3 ceilometer. CPC measurements within the liquid-containing cloud layer have been blacked out due to the possibility of contamination within this layer.

flights included the operation of the National Center for Atmospheric Research (NCAR) Video Particle Sampler (VIPS) probe (Schmitt et al. 2013). VIPS, operated as a guest instrument, provided information on ice hydrometeor size distributions (20–2,000 μm) and crystal habit and aspect ratio. Figure 2d shows an example of such measurements from 21 October 2016 (0015–0030 UTC), illustrating a representative sample of ice crystals from the cloud and precipitation regime in which the balloon was operating. Such in situ measurements provide information that can, through process studies, connect surface-based remote sensing retrievals to understanding cloud water budgets through the evaluation of ice crystal size and fall speed. These specific measurements were subsequently used for the initial verification of polarimetric radar-based estimates of particle shapes (Matrosov et al. 2017), which could be applied to longer time scales to enhance our cloud process understanding.

Atmospheric turbulence plays a significant role in modifying the vertical distribution and transport of aerosol particles, liquid water, ice crystals, heat, moisture, and other atmospheric constituents. Generation of turbulence occurs via a combination of mechanical forcing as air flows over the surface, surface heating, cloud diabatic heating, and/or mesoscale dynamics, all of which are modulated by atmospheric stratification. The ability to understand vertical profiles of turbulence is essential for supporting process-based understanding of the Arctic system. During October 2016 ICARUS TBS flights, in situ measurements of turbulence were made using a 3D sonic anemometer installed in an aerofoil housing. An example profile of turbulent dissipation rates derived on 20 October demonstrates how turbulent mixing and atmospheric stability are related (Fig. 2e). Here, the lower atmosphere was very stable, resulting in small dissipation rates except for in the shallow surface mixed layer, where mechanical mixing led to larger dissipation rates. Such measurements are useful for developing retrievals of turbulence from ground-based remote sensors (O'Connor et al. 2010; Shupe et al. 2012), which can then be used to provide continuous turbulence statistics. When flown together with aerosol or cloud sensors, such instrumentation additionally supports examinations of processes related to cloud-driven mixing, aerosol–cloud interaction, and the impact of embedded stable layers on vertical transport processes.

LOOKING AHEAD. *Advancing capabilities.* Currently, atmospheric properties are measured by ARM using the DH2 UAS and TBS platforms. To build upon these capabilities, ARM is expanding its unmanned infrastructure to include new platforms and instrumentation. The recent addition of a Navmar Applied Sciences Corporation TigerShark Block 3 XP-AR, dubbed the ArcticShark, significantly expands the ARM UAS flight range and operating conditions. This aircraft and its mobile operations center have been hardened specifically for cold-temperature operation to accommodate the Oliktok Point environment. With a wingspan of 6.5 m and a maximum gross takeoff weight of 295 kg, it is capable of flight up to 5.5 km above sea level over ranges of up to 500 km and has an 8-h maximum endurance. Its relatively slow 30–40 m s^{-1} airspeed allows for low-speed sampling of the atmosphere. The system can be operated under surface winds up to 12.9 m s^{-1} with a maximum 5.1 m s^{-1} tailwind and a 7.7 m s^{-1} crosswind component. Its 85-L interior payload volume and four wing-mounted pylons make it capable of carrying a variety of sensors and probes in payload configurations up to 46 kg (Fig. 6). The ArcticShark will carry a combination of instruments operated in house by the ARM Aerial Facility (AAF) and guest instruments integrated for specific field campaigns.

Taking advantage of instrumentation miniaturization efforts, ARM has a variety of instruments available for use on the ArcticShark and/or TBSs (Table 2). This includes sensors for observing the atmospheric state and thermodynamics (temperature, pressure, humidity, three-dimensional wind, and gas concentrations), up- and downwelling broadband infrared and solar radiation, surface temperature, aerosol number concentration, aerosol size distribution, aerosol absorption, aerosol composition (filter samples), cloud-droplet size distribution, and cloud liquid water content. These capabilities were selected through discussions with the research community and are based in part on guidance from the ARM Aerial Needs Workshop report (DOE 2015b) and ARM Unmanned Aerial Systems Implementation Plan (DOE 2015a), published in October 2015 and November 2016, respectively. To ensure scientifically relevant measurements, ARM has been working with university, industry, and national laboratory partners to characterize the performance of the instruments deployed and improve the integration of these sensors on ARM-operated platforms.

Fig. 6. The DOE ARM ArcticShark.

As discussed briefly in the preceding section, the Arctic offers a challenging environment for operation of UASs and TBSs. Strong winds, icing, and limited visibility all negatively impact such activities. While the physical limitations for the operation of specific vehicles are strongly tied to the vehicles and platforms, the availability of restricted airspace offers the possibility for operations that are challenging to conduct within the current FAA regulatory environment. Any flights proposed need to undergo a safety review conducted by Sandia National Laboratories and the Department of Energy, but activities deemed safe and appropriate by these entities are allowable within R-2204. Additionally, DOE is working with industry and agency partners to develop technologies to help mitigate some of these issues. As an example, ongoing work with the National Aeronautics and Space Administration (NASA), NOAA, universities, and industry is evaluating aircraft icing and mitigation techniques for the ArcticShark and DataHawk2.

Community access. The DOE ARM program is a science user facility supporting the atmospheric science community through the production of both baseline and field campaign observations. UAS operations at Oliktok Point have included both of these activity classes. The establishment of restricted and warning areas around Oliktok Point has attracted various groups to request access to this airspace for UAS development and science missions. Meanwhile, the operation of ARM-managed DH2 UASs and TBSs throughout ICARUS represents an emerging ARM baseline measurement. ICARUS, along with subsequent baseline operations, is designed to collect observations of the Arctic environment spanning the annual cycle to the extent practical.

To support such an effort, ARM has hired and trained personnel to operate the UASs and TBSs. While these operators are not permanently stationed at Oliktok Point, they have become familiar with the site and have operated there regularly through participation in the above (and additional) field campaigns. Requirements of each specific mission detail the exact number of people required for the operation of a given platform, with a minimum of two operators and a range safety officer required to operate either one. The extent to which routine operations can allow for continuous sampling is limited by the weather conditions and the number of operators available. For example, high winds (>10–15 m s^{-1}) pose a significant

Table 2. List of ArcticShark/TBS instruments operated by the AAF.

Instrument		Measurement	Manufacturer
Aerosol Counting, Composition, Extinction and Sizing System (ACCESS)	Filter sampler	Aerosol samples	Brechtel
	Mixing Condensation Particle Counter (MCPC)	Aerosol concentration (>7 nm)	
	Miniaturized Optical Particle Counter (mOPC)	Aerosol size distribution (0.18–10 μm)	
	Single Channel Tricolor Absorption Photometer (STAP)	Aerosol light absorption	
POPS		Aerosol size distribution (0.15–3 μm)	Handix Scientific
CDP		Cloud drop size distribution (2–50 μm)	DMT
Aircraft-Integrated Meteorological Measurement System (AIMMS-30)		Pressure, temperature, relative humidity, wind	Avantech Research Inc.
VN-300		Aircraft heading, position, attitude	VectorNav
HS-2000DP		Temperature, relative humidity	Procon
Sunshine Pyranometer (SPN-1)		Broadband irradiance (400–2,700 nm)	Delta-T
IR20		Broadband irradiance (4.5–40 μm)	Hukseflux
CT09		Infrared (8–14 μm) temperature	Heitronics
LI-840a		CO_2/H_2O gas concentration	LI-COR

hurdle to currently operated systems. Additionally, limited visibility and the threat of icing can reduce the reach and deployability of UAS. Finally, extreme winter cold, while not insurmountable operationally, can impact operations both from systems performance and operator safety perspectives. While in theory operation in R-2204 can offer opportunities for nighttime and beyond-visual-line-of-sight (BVLOS) operations, such activities still need to be approved by the DOE before they are allowable.

ARM data services include data collection, archival, integration, analysis, and discovery (McCord and Voyles 2016), and are an essential element of ARM's infrastructure. Observations collected with the DH2 and the TBSs are considered part of ARM's aerial measurements and use a unique data collection process. From ICARUS onward, ARM staff have monitored the successful collection of data during flights and continue to work alongside the ARM Data Management Facility (DMF) to implement and monitor the flow of UAS and TBS data to the DMF. After raw data are delivered, the Data Quality Office (Peppler et al. 2016) and instrument mentors process the data to assess instrument performance, data quality, and uncertainty. In parallel with the above activities, DMF developers work with mentors to assess the quality control and processing level of the data and its readiness for release. Once released, users can freely access UAS and TBS data, along with that from other ARM instrumentation, through the ARM Data Discovery website (www.arm.gov/data).

Access to the ARM-managed airspace is obtained through the proposal of custom field campaign activities in conjunction with ARM sites and the development and approval of an aviation safety plan. Such proposals can be submitted as an intensive operation period (IOP) request (www.arm.gov/research/campaign-proposal) to the ARM program. Field campaign proposals are accepted at any time, with larger field campaigns [budgets exceeding $300,000 (U.S. dollars)] reviewed once per year and smaller campaigns reviewed quarterly. With the maturation of ARM-managed UAS and TBS platforms, ARM is now accepting proposals from the science community to deploy the tethered balloon at Oliktok and ARM DH2s at any ARM site. Currently, ARM plans to make the ArcticShark available for user proposals in 2019.

SUMMARY. UAS and TBS operations at Oliktok Point, Alaska, have laid the groundwork for extended and semiroutine operations of such vehicles by the DOE ARM program. This paper provided an overview of these activities, along with insights into obstacles overcome and initial science achieved. While measurements from these initial activities are just beginning to be analyzed, these observations demonstrate the value of the new perspectives offered by these platforms, including information on spatial variability and vertical structure, and over difficult-to-sample surfaces such as newly forming sea ice and partially frozen tundra. Over the next few years, the measurements obtained, and those to be collected in the near future, will continue to be analyzed and used for model and remote sensing retrieval development and for the production of scientific understanding. Some such studies are currently being prepared for publication, offering new insights into atmospheric thermodynamic structure, aerosol processes, cloud macro- and microphysics, and turbulent and radiative energy fluxes at high latitudes. Information gained on the efficient use of unmanned platforms in the Arctic will benefit future missions, while scientific insight from such activities will continue, providing a valuable complement to measurements obtained from ARM's surface-based sensors and those provided by crewed research aircraft and satellites.

ACKNOWLEDGMENTS. This work is supported by the U.S. Department of Energy and NOAA. This includes support through grants and cooperative agreements (DOE Office of Science Project Numbers DE-SC0011459, DE-SC0013306, and DE-SC0014568), and through direct funding of the Atmospheric Radiation Measurement program and the NOAA Physical Sciences Division and NOAA Chemical Sciences Division. The authors would like to specifically recognize the efforts of the Oliktok Point site technicians, who work throughout the year in extremely harsh conditions to keep the facility operating, and work diligently with UAS and TBS operators to ensure safe and successful operations. Additionally, we would like to recognize work completed by the pilots, engineers, and research staff of the University of Colorado's Research and Engineering Center for Unmanned Vehicles (RECUV), and Integrated Remote and In Situ Sensing Program (IRISS), to prepare and deploy unmanned aircraft for the campaigns discussed in the manuscript. Finally, we recognize the National Center for Atmospheric Research (NCAR) for providing instrumentation during the ERASMUS campaign and assisting with the evaluation and calibration of sensors.

REFERENCES

Burek, K. A., F. M. D. Gulland, and T. M. O'Hara, 2008: Effects of climate change on Arctic marine mammal health. *Ecol. Appl.*, **18**, S126–S134, https://doi.org/10.1890/06-0553.1.

Cassano, J. J., J. A. Maslanik, C. J. Zappa, A. L. Gordon, R. I. Cullather, and S. L. Knuth, 2010: Observations of Antarctic polynya with unmanned aircraft systems. *Eos, Trans. Amer. Geophys. Union*, **91**, 245–246, https://doi.org/10.1029/2010EO280001.

Chylek, P., T. J. Vogelsang, J. D. Klett, N. Hengartner, D. Higdon, G. Lesins, and M. K. Dubey, 2016: CMIP5 models' projected Arctic warming. *J. Climate*, **29**, 1417–1428, https://doi.org/10.1175/JCLI-D-15-0362.1.

Corrigan, C., V. Ramanathan, M. V. Ramana, D. Kim, and G. Roberts, 2006: Chasing black carbon using autonomous unmanned aerial vehicles. *Eos, Trans. Amer. Geophys. Union*, **87** (Fall Meeting Suppl.), Abstract A43A-0106.

Cox, C. J., T. Uttal, C. N. Long, M. D. Shupe, R. S. Stone, and S. Starkweather, 2016: The role of springtime Arctic clouds in determining autumn sea ice extent. *J. Climate*, **29**, 6581–6596, https://doi.org/10.1175/JCLI-D-16-0136.1.

Creamean, J. M., M. Maahn, G. de Boer, A. McComiskey, A. J. Sedlacek, and Y. Feng, 2018: The influence of local oil exploration and regional wildfires on summer 2015 aerosol over the North Slope of Alaska. *Atmos. Chem. Phys.*, **18**, 555–570, https://doi.org/10.5194/acp-18-555-2018.

Curry, J. A., J. Maslanik, G. J. Holland, and J. Pinto, 2004: Applications of aerosondes in the Arctic. *Bull. Amer. Meteor. Soc.*, **85**, 1855–1861, https://doi.org/10.1175/BAMS-85-12-1855.

de Boer, G., H. Morrison, M. D. Shupe, and R. Hildner, 2011: Evidence of liquid dependent ice nucleation in high-latitude stratiform clouds from surface remote sensors. *Geophys. Res. Lett.*, **38**, L01803, https://doi.org/10.1029/2010GL046016.

——, W. Chapman, J. E. Kay, B. Medeiros, M. D. Shupe, S. Vavrus, and J. Walsh, 2012: A characterization of the present-day Arctic atmosphere in CCSM4. *J. Climate*, **25**, 2676–2695, https://doi.org/10.1175/JCLI-D-11-00228.1.

——, M. D. Ivey, B. Schmid, S. McFarlane, and R. Petty, 2016a: Unmanned platforms monitor the Arctic atmosphere. *Eos, Trans. Amer. Geophys. Union*, **97**, https://doi.org/10.1029/2016EO046441.

——, and Coauthors, 2016b: The Pilatus unmanned aircraft system for lower atmospheric research. *Atmos. Meas. Tech.*, **9**, 1845–1857, https://doi.org/10.5194/amt-9-1845-2016.

DOE, 2015a: Accelerated Climate Modeling for Energy (ACME)–Atmospheric Radiation Measurement (ARM) Climate Research Facility–Atmospheric System Research (ASR) Coordination Workshop. Dept. of Energy Rep. DOE/SC-0182, 53 pp., https://science.energy.gov/~/media/ber/pdf/workshop%20reports/CESD_ACME_ARM_ASR_workshopreport_web.pdf.

——, 2015b: Aerial Observation Needs Workshop. Dept. of Energy Rep. DOE/SC-0179, 48 pp., https://science.energy.gov/~/media/ber/pdf/workshop%20reports/CESD_AerialObsNeeds_Workshop_2015web.pdf.

Dong, X., B. Xi, K. Crosby, C. N. Long, R. S. Stone, and M. D. Shupe, 2010: A 10-year climatology of Arctic cloud fraction and radiative forcing at Barrow, Alaska. *J. Geophys. Res.*, **115**, D17212, https://doi.org/10.1029/2009JD013489.

Döscher, R., T. Vihma, and E. Maksimivich, 2014: Recent advances in understanding the Arctic climate system state and change from a sea ice perspective: A review. *Atmos. Chem. Phys.*, **14**, 10 929–10 999, https://doi.org/10.5194/acpd-14-10929-2014.

Duda, D. P., G. L. Stephens, and S. K. Cox, 1991: Microphysical and radiative properties of marine stratocumulus from tethered balloon measurements. *J. Appl. Meteor. Climatol.*, **30**, 170–186, https://doi.org/10.1175/1520-0450(1991)030<0170:MARPOM>2.0.CO;2.

Gao, R. S., and Coauthors, 2016: A light-weight, high-sensitivity particle spectrometer for PM2.5 aerosol measurements. *Aerosol Sci. Technol.*, **50**, 88–99, https://doi.org/10.1080/02786826.2015.1131809.

Garrett, T. J., and C. Zhao, 2006: Increased Arctic cloud longwave emissivity associated with pollution from mid-latitudes. *Nature*, **440**, 787–789, https://doi.org/10.1038/nature04636.

Greenberg, J., 1999: Tethered balloon measurements of biogenic VOCs in the atmospheric boundary layer. *Atmos. Environ.*, **33**, 855–867, https://doi.org/10.1016/S1352-2310(98)00302-1.

Hansen, J., and L. Nazarenko, 2004: Soot climate forcing via snow and ice albedos. *Proc. Natl. Acad. Sci. USA*, **101**, 423–428, https://doi.org/10.1073/pnas.2237157100.

Hill, G. E., and D. S. Woffinden, 1980: A balloonborne instrument for the measurement of vertical profiles of supercooled liquid water concentration. *J. Appl. Meteor.*, **19**, 1285–1292, https://doi.org/10.1175/1520-0450(1980)019<1285:ABIFTM>2.0.CO;2.

Holland, G. J., T. McGeer, and H. Youngren, 1992: Autonomous aerosondes for economical atmospheric soundings anywhere on the globe. *Bull. Amer. Meteor. Soc.*, **73**, 1987–1998, https://doi.org/10.1175/1520-0477(1992)073<1987:AAFEAS>2.0.CO;2.

——, and Coauthors, 2001: The Aerosonde robotic aircraft: A new paradigm for environmental observations. *Bull. Amer. Meteor. Soc.*, **82**, 889–901,

https://doi.org/10.1175/1520-0477(2001)082<0889:TARAAN>2.3.CO;2.

Houston, A. L., B. Argrow, J. Elston, J. Lahowetz, E. W. Frew, and P. C. Kennedy, 2012: The Collaborative Colorado–Nebraska Unmanned Aircraft System Experiment. *Bull. Amer. Meteor. Soc.*, **93**, 39–54, https://doi.org/10.1175/2011BAMS3073.1.

Kay, J. E., T. L'Ecuyer, A. Gettelman, G. Stephens, and C. O'Dell, 2008: The contribution of cloud and radiation anomalies to the 2007 sea ice extent minimum. *Geophys. Res. Lett.*, **35**, L08503, https://doi.org/10.1029/2007GL032628.

Kitchen, M., and S. J. Caughey, 1981: Tethered-balloon observations of the structure of small cumulus clouds. *Quart. J. Roy. Meteor. Soc.*, **107**, 853–874, https://doi.org/10.1002/qj.49710745407.

Knuth, S. L., and J. J. Cassano, 2014: Estimating sensible and latent heat fluxes using the integral method from in situ aircraft measurements. *J. Atmos. Oceanic Technol.*, **31**, 1964–1981, https://doi.org/10.1175/JTECH-D-14-00008.1.

Kollias, P., and Coauthors, 2016: Development and applications of ARM millimeter-wavelength cloud radars. *The Atmospheric Radiation Measurement (ARM) Program: The First 20 Years*, *Meteor. Monogr.*, No. 57, Amer. Meteor. Soc., https://doi.org/10.1175/AMSMONOGRAPHS-D-15-0037.1.

Kwok, R., and N. Untersteiner, 2011: The thinning of Arctic sea ice. *Phys. Today*, **64**, 36–41, https://doi.org/10.1063/1.3580491.

Langford, J. S., and K. A. Emanuel, 1993: An unmanned aircraft for dropwindsonde deployment and hurricane reconnaissance. *Bull. Amer. Meteor. Soc.*, **74**, 367–375, https://doi.org/10.1175/1520-0477(1993)074<0367:AUAFDD>2.0.CO;2.

Lawrence, D. A., and B. B. Balsley, 2013: High-resolution atmospheric sensing of multiple atmospheric variables using the DataHawk small airborne measurement system. *J. Atmos. Oceanic Technol.*, **30**, 2352–2366, https://doi.org/10.1175/JTECH-D-12-00089.1.

Lindsay, R., and A. Schweiger, 2015: Arctic sea ice thickness loss determined using subsurface, aircraft, and satellite observations. *Cryosphere*, **9**, 269–283, https://doi.org/10.5194/tc-9-269-2015.

Long, C. N., A. Bucholtz, H. Jonsson, B. Schmid, A. Vogelmann, and J. Wood, 2010: A method of correcting for tilt from horizontal in downwelling SW measurements on moving platforms. *Open Atmos. Sci. J.*, **4**, 78–87, https://doi.org/10.2174/1874282301004010078.

Lubin, D., and A. M. Vogelmann, 2006: A climatologically significant aerosol longwave indirect effect in the Arctic. *Nature*, **439**, 453–456, https://doi.org/10.1038/nature04449.

Maahn, M., G. de Boer, J. M. Creamean, G. Feingold, G. M. McFarquhar, W. Wu, and F. Mei, 2017: The observed influence of local anthropogenic pollution on northern Alaskan cloud properties. *Atmos. Chem. Phys.*, **17**, 142709–142726, https://doi.org/10.5194/acp-17-14709-2017.

Maslanik, J., J. Stroeve, C. Fowler, and W. Emery, 2011: Distribution and trends in Arctic sea ice age through spring 2011. *Geophys. Res. Lett.*, **38**, L13502, https://doi.org/10.1029/2011GL047735.

Matrosov, S. Y., C. G. Schmitt, M. Maahn, and G. de Boer, 2017: Atmospheric ice particle shape estimates from polarimetric radar measurements and in situ observations. *J. Atmos. Oceanic Technol.*, **34**, 2569–2587, https://doi.org/10.1175/JTECH-D-17-0111.1.

McComiskey, A., and R. A. Ferrare, 2016: Aerosol physical and optical properties and processes in the ARM program. *The Atmospheric Radiation Measurement (ARM) Program: The First 20 Years*, *Meteor. Monogr.*, No. 57, Amer. Meteor. Soc., https://doi.org/10.1175/AMSMONOGRAPHS-D-15-0028.1.

McCord, R., and J. Voyles, 2016: The ARM Data System and archive. *The Atmospheric Radiation Measurement (ARM) Program: The First 20 Years*, *Meteor. Monogr.*, No. 57, Amer. Meteor. Soc., https://doi.org/10.1175/AMSMONOGRAPHS-D-15-0043.1.

Miller, N. B., M. D. Shupe, J. T. M. Lenaerts, J. E. Kay, G. de Boer, and R. Bennartz, 2018: Process-based model evaluation using surface energy budget observations in central Greenland. *J. Geophys. Res. Atmos.*, **123**, https://doi.org/10.1029/2017JD027377.

Morrison, H., and Coauthors, 2009: Intercomparison of model simulations of mixed-phase clouds observed during the ARM Mixed-Phase Arctic Cloud Experiment. II: Multilayer cloud. *Quart. J. Roy. Meteor. Soc.*, **135**, 1003–1019, https://doi.org/10.1002/qj.415.

Neff, W., D. Helmig, A. Grachev, and D. Davis, 2008: A study of boundary layer behavior associated with high NO concentrations at the South Pole using a minisodar, tethered balloon, and sonic anemometer. *Atmos. Environ.*, **42**, 2762–2779, https://doi.org/10.1016/j.atmosenv.2007.01.033.

O'Connor, E. J., A. J. Illingworth, I. M. Brooks, C. D. Westbrook, R. J. Hogan, F. Davies, and B. J. Brooks, 2010: A method for estimating the turbulent kinetic energy dissipation rate from a vertically pointing Doppler lidar, and independent evaluation from balloon-borne in situ measurements. *J. Atmos. Oceanic Technol.*, **27**, 1652–1664, https://doi.org/10.1175/2010JTECHA1455.1.

Penner, J. E., X. Q. Dong, and Y. Chen, 2004: Observational evidence of a change in radiative forcing due to the indirect aerosol effect. *Nature*, **427**, 231–234, https://doi.org/10.1038/nature02234.

Peppler, R. A., K. E. Kehoe, J. W. Monroe, and A. K. Theisen, 2016: The ARM data quality program. *The Atmospheric Radiation Measurement (ARM) Program: The First 20 Years*, *Meteor. Monogr.*, No. 57, Amer. Meteor. Soc., https://doi.org/10.1175/AMSMONOGRAPHS-D-15-0039.1.

Pisano, J. T., I. McKendry, D. G. Steyn, and D. R. Hastie, 1997: Vertical nitrogen dioxide and ozone concentrations measured from a tethered balloon in the lower Fraser valley. *Atmos. Environ.*, **31**, 2071–2078, https://doi.org/10.1016/S1352-2310(96)00146-X.

Pithan, F., and T. Mauritsen, 2014: Arctic amplification dominated by temperature feedbacks in contemporary climate models. *Nat. Geosci.*, **7**, 181–184, https://doi.org/10.1038/ngeo2071.

Post, E., and Coauthors, 2013: Ecological consequences of sea ice decline. *Science*, **341**, 519–524, https://doi.org/10.1126/science.1235225.

Quinn, P. K., T. L. Miller, T. S. Bates, J. A. Ogren, E. Andrews, and G. E. Shaw, 2002: A 3-year record of simultaneously measured aerosol chemical and optical properties at Barrow, Alaska. *J. Geophys. Res.*, **107**, 4130, https://doi.org/10.1029/2001JD001248.

——, T. S. Bates, K. Schulz, and G. E. Shaw, 2009: Decadal trends in aerosol chemical composition at Barrow, Alaska: 1976–2008. *Atmos. Chem. Phys.*, **9**, 8883–8888, https://doi.org/10.5194/acp-9-8883-2009.

Ramanathan, V., M. V. Ramana, G. Roberts, D. Kim, C. Corrigan, C. Chung, and D. Winker, 2007: Warming trends in Asia amplified by brown cloud solar absorption. *Nature*, **448**, 575–579, https://doi.org/10.1038/nature06019.

Rigor, I. G., R. L. Colony, and S. Martin, 2000: Variations in surface air temperature observations in the Arctic, 1979–97. *J. Climate*, **13**, 896–914, https://doi.org/10.1175/1520-0442(2000)013<0896:VISATO>2.0.CO;2.

Romanovsky, V. E., M. Burgess, M. Smith, K. Yoshikawa, and J. Brown, 2002: Permafrost temperature records: Indicators of climate change. *Eos, Trans. Amer. Geophys. Union*, **83**, 589–594, https://doi.org/10.1029/2002EO000402.

Schmid, B., R. G. Ellingson, and G. M. McFarquhar, 2016: ARM aircraft measurements. *The Atmospheric Radiation Measurement (ARM) Program: The First 20 Years*, *Meteor. Monogr.*, No. 57, Amer. Meteor. Soc., https://doi.org/10.1175/AMSMONOGRAPHS-D-15-0042.1.

Schmitt, C. G., M. Stuefer, A. J. Heymsfield, and C. K. Kim, 2013: The microphysics of ice fog measured in urban environments in interior Alaska. *J. Geophys. Res. Atmos.*, **118**, 112136–112147, https://doi.org/10.1002/jgrd.50822.

Screen, J. A., and I. Simmonds, 2010: The central role of diminishing sea ice in recent Arctic temperature amplification. *Nature*, **464**, 1334–1337, https://doi.org/10.1038/nature09051.

Serreze, M. C., and J. A. Francis, 2006: The Arctic amplification debate. *Climatic Change*, **76**, 241–264, https://doi.org/10.1007/s10584-005-9017-y.

——, and R. G. Barry, 2011: Processes and impacts of Arctic amplification: A research synthesis. *Global Planet. Change*, **77**, 85–96, https://doi.org/10.1016/j.gloplacha.2011.03.004.

Shupe, M. D., 2011: Clouds at Arctic atmospheric observatories. Part II: Thermodynamic phase characteristics. *J. Appl. Meteor. Climatol.*, **50**, 645–661, https://doi.org/10.1175/2010JAMC2468.1.

——, V. P. Walden, E. Eloranta, T. Uttal, J. R. Campbell, S. M. Starkweather, and M. Shiobara, 2011: Clouds at Arctic atmospheric observatories. Part I: Occurrence and macrophysical properties. *J. Appl. Meteor. Climatol.*, **50**, 626–644, https://doi.org/10.1175/2010JAMC2467.1.

——, I. M. Brooks, and G. Canut, 2012: Evaluation of turbulent dissipation rate retrievals from Doppler cloud radar. *Atmos. Meas. Tech.*, **5**, 1375–1385, https://doi.org/10.5194/amt-5-1375-2012.

——, P. O. G. Person, I. M. Brooks, M. Tjernström, J. Sedlar, T. Mauritsen, S. Sjogren, and C. Leck, 2013: Cloud and boundary layer interactions over the Arctic sea-ice in late summer. *Atmos. Chem. Phys.*, **13**, 9379–9400, https://doi.org/10.5194/acp-13-9379-2013.

Simon, C., L. Arris, and B. Heal, 2005: *Arctic Climate Impact Assessment*. Cambridge University Press, 1020 pp.

Stephens, G. L., and Coauthors, 2000: The Department of Energy's Atmospheric Radiation Measurement (ARM) Unmanned Aerospace Vehicle (UAV) program. *Bull. Amer. Meteor. Soc.*, **81**, 2915–2938, https://doi.org/10.1175/1520-0477(2000)081<2915:TDOESA>2.3.CO;2.

Stroeve, J., M. M. Holland, W. Meier, T. Scambos, and M. Serreze, 2007: Arctic sea ice decline: Faster than forecast. *Geophys. Res. Lett.*, **34**, L09501, https://doi.org/10.1029/2007GL029703.

——, V. Kattsov, A. Barrett, M. Serreze, T. Pavlova, M. Holland, and W. N. Meier, 2012: Trends in Arctic sea ice extent from CMIP5, CMIP3 and observations. *Geophys. Res. Lett.*, **39**, L16502, https://doi.org/10.1029/2012GL052676.

Sullivan, P. P., J. C. Weil, E. G. Patton, H. J. Jonker, and D. V. Mironov, 2016: Turbulent winds and temperature fronts in large-eddy simulations of the stable atmospheric boundary layer. *J. Atmos. Sci.*, **73**, 1815–1840, https://doi.org/10.1175/JAS-D-15-0339.1.

Telg, H., D. M. Murphy, T. S. Bates, J. E. Johnson, P. K. Quinn, F. Giardi, and R. S. Gao, 2017: A practical set of miniaturized instruments for vertical profiling of aerosol physical properties. *Aerosol Sci. Technol.*, **51**, 715–723, https://doi.org/10.1080/02786826.2017.1296103.

Turner, D. D., and U. Löhnert, 2014: Information content and uncertainties in thermodynamic profiles and liquid cloud properties retrieved from the ground-based Atmospheric Emitted Radiance Interfereometer (AERI). *J. Appl. Meteor. Climatol.*, **53**, 752–771, https://doi.org/10.1175/JAMC-D-13-0126.1.

——, and R. G. Ellingson, Eds., 2016: *The Atmospheric Radiation Measurement (ARM) Program: The First 20 Years. Meteor. Monogr.*, No. 57, Amer. Meteor. Soc.

Tyler, S. W., J. S. Selker, M. B. Hausner, C. E. Hatch, T. Torgersen, C. E. Thodal, and S. G. Schladow, 2009: Environmental temperature sensing using Raman spectra DTS fiber-optic methods. *Water Resour. Res.*, **45**, W00D23, https://doi.org/10.1029/2008WR007052.

Uttal, T., and Coauthors, 2016: International Arctic Systems for Observing the Atmosphere: An International Polar Year legacy consortium. *Bull. Amer. Meteor. Soc.*, **97**, 1033–1056, https://doi.org/10.1175/BAMS-D-14-00145.1.

Van den Kroonenberg, A., T. Martin, M. Buschmann, J. Bange, and P. Vorsmann, 2008: Measuring the wind vector using the autonomous mini aerial vehicle M^2AV. *J. Atmos. Oceanic Technol.*, **25**, 1969–1982, https://doi.org/10.1175/2008JTECHA1114.1.

Verlinde, J., 2010: The Arctic Lower Troposphere Observed Structure (ALTOS) campaign. Dept. of Energy Rep. DOE/SC-ARM-10-034, 4 pp., www.arm.gov/publications/programdocs/doe-sc-arm-10-034.pdf.

——, and Coauthors, 2007: The Mixed-Phase Arctic Cloud Experiment. *Bull. Amer. Meteor. Soc.*, **88**, 205–221, https://doi.org/10.1175/BAMS-88-2-205.

——, B. D. Zak, M. D. Shupe, M. D. Ivey, and K. Stamnes, 2016: The ARM North Slope of Alaska (NSA) sites. *The Atmospheric Radiation Measurement (ARM) Program: The First 20 Years*, *Meteor. Monogr.*, No. 57, Amer. Meteor. Soc., https://doi.org/10.1175/AMSMONOGRAPHS-D-15-0023.1.

Xie, S., S. A. Klein, J. J. Yio, A. C. M. Beljaars, C. N. Long, and M. Zhang, 2006: An assessment of ECMWF analyses and model forecasts over the North Slope of Alaska using observations from the ARM Mixed-Phase Arctic Cloud Experiment. *J. Geophys. Res.*, **111**, D05107, https://doi.org/10.1029/2005JD006509.

Zhang, T., S. A. Bowling, and K. Stamnes, 1997: Impact of the atmosphere on surface radiative fluxes and snowmelt in the Arctic and subarctic. *J. Geophys. Res.*, **102**, 4287–4302, https://doi.org/10.1029/96JD02548.